

# A spatially dependent correction of Gaia EDR3 parallax zero-point offset based on 0.3 million LAMOST DR8 giant stars

CHUN WANG,<sup>1,\*</sup> HAIBO YUAN,<sup>2</sup> AND YANG HUANG<sup>3</sup>

<sup>1</sup>*Tianjin Astrophysics Center, Tianjin Normal University, Tianjin 300387, People's Republic of China.*

<sup>2</sup>*Department of Astronomy, Beijing Normal University, Beijing 100875, People's Republic of China.*

<sup>3</sup>*South-Western Institute for Astronomy Research, Yunnan University, Kunming, Yunnan 650091, People's Republic of China.*

## ABSTRACT

We have studied the zero-point offset of Gaia early Data Release 3 (EDR3) parallaxes based on a sample of 0.3 million giant stars built from the LAMOST data with distance accuracy better than 8.5%. The official parallax zero-point corrections largely reduce the global offset in the Gaia EDR3 parallaxes: the global parallax offsets are  $-27.9 \mu\text{as}$  and  $-26.5 \mu\text{as}$  (before correction) and  $+2.6 \mu\text{as}$  and  $+2.9 \mu\text{as}$  (after correction) for the five- and six-parameter solutions, respectively. The bias of the raw parallax measurements is significantly dependent on the  $G$  magnitudes, spectral colors, and positions of stars. The official parallax zero-point corrections could reduce parallax bias patterns with  $G$  magnitudes, while could not fully account the patterns in the spaces of the spectral colors and positions. In the current paper, a spatially dependent parallax zero-point correction model for Gaia EDR3 five-parameter solution in the LAMOST footprint is firstly provided with the advantage of huge number of stars in our sample.

## 1. INTRODUCTION

Gaia Early Data Release 3 (Gaia Collaboration et al. 2021) have released astrometric and photometric data for over 1.8 billion sources based on observations from the first 34 months (from 2014 July to 2017 May) by the European Space Agency's Gaia mission (Gaia Collaboration et al. 2016). Among of them, 1.468 billion sources have full astrometric data, including position, parallax, and proper motions. The data set of Gaia EDR3 is widely used in the fields of the stellar and Galactic astrophysics.

In Gaia EDR3, the typical uncertainties of parallaxes are 0.03–1.4 mas for stars with  $15 < G < 21$  mag (Gaia Collaboration et al. 2021). The systematic parallax errors are inevitable because of the imperfections in the instruments and data processing (Lindgren et al. 2021a), which will produce large systematic distance errors especially for more distant stars. Thus, investigating the systematic bias of the Gaia EDR3 parallax is important for its further applications. Lindgren et al. (2021b) have constructed a parallax zero-point correction model, which is a function of the  $G$ -band magnitude, spectral shape (colors), and ecliptic latitude of the sources. This correction model is based on quasars distributed across the entire sky, binary stars, and stars in the Large Magellanic Cloud (LMC). The correction models are different for sources with five- and six-parameter solutions. However, the correction models are mostly appropriate for only sources having similar magnitudes and colors to quasars. Thus the independent test of parallax zero-point offsets of Gaia EDR3 using Galactic stars is needed. Several papers have also contributed to the parallax zero-point offset of Gaia EDR3 estimates using different tracers, including quasars, RR Lyrae stars, red clump stars, red giant stars and binaries (Bhardwaj et al. 2021; Liao et al. 2021; Groenewegen 2021; El-Badry et al. 2021; Stassun & Torres 2021; Zinn 2021; Huang et al. 2021; Ren et al. 2021). Amongst of them, Huang et al. (2021) and Ren et al. (2021) estimate the independent parallax zero-point offsets of Gaia EDR3 using  $\sim 0.07$  million LAMOST primary red clump (PRC) stars and  $\sim 0.11$  million W Ursae Majoris (EW)-type eclipsing binary systems in a wide magnitude and color ranges with the advantage of large stellar sample and their accurate measurements of distance. They find  $\sim -27 \mu\text{as}$  and  $\sim +4 \mu\text{as}$  global zero-point offset of Gaia EDR3 parallaxes before and after correction, respectively. The official parallax zero-point model of Lindgren et al. (2021b) could reduce the global bias in the Gaia EDR3 parallax. After

\* Corresponding author (wchun@tjnu.edu.cn)

correction, the parallax bias variations with spectral colors and positions still exist. Thus, it is useful to investigate the zero-point offset in Gaia EDR3 parallaxes, especially the parallax zero-point offset variations with the positions.

Here, we use the sources targeted by LAMOST to investigate the zero-point offset in Gaia EDR3 parallaxes. We will introduce our data set in Section 2. The main results are presented and discussed in Section 3. Finally, Section 4 presents a summary of our results.

## 2. DATA

We use the data of the value-added catalog for LAMOST DR8 low resolution spectra (Wang et al. 2022, accepted) to test the zero-point offset of Gaia EDR3. The catalog contains accurate photometric distances for about 7.1 million spectra of 5.17 million unique stars with spectral signal-to-noise ratios (SNRs) higher than 10 obtained by the Large Sky Area Multi-Object Fibre Spectroscopic Telescope (LAMOST) Galactic spectroscopic surveys (Deng et al. 2012; Zhao et al. 2012; Liu et al. 2014). The photometric distance of individual stars observed by LAMOST are estimated with distance modulus method using the 2MASS (Skrutskie et al. 2006)  $K_s$  band apparent magnitudes, interstellar extinctions and 2MASS  $K_s$  band absolute magnitudes ( $M_{K_s}$ ) derived directly from the LAMOST spectra using neural network models. The photometric distance is accurate to 8.5% for stars with spectral SNRs larger than 50. Especially, the photometric distance show small dependence on the apparent magnitudes, positions of stars, absolute magnitudes and spectral colors. It is a suitable dataset to test the zero-point offset in Gaia EDR3 parallaxes.

### 2.1. Sample selection

We cross-match the value-added catalog with Gaia EDR3 and 2MASS, and use the following criteria to select stellar sample to test the zero-point offset of Gaia EDR3 parallax:

- LAMOST spectral signal to noise ratio (SNR)  $\geq 50$ , parallaxes smaller than 1.5 mas, surface gravity  $\log g \leq 3.8$ , and the uncertainty of 2MASS  $K_s$  band apparent magnitude smaller than 0.03 mag.
- The renormalized unit weight error (RUWE)  $\leq 1.4$ .
- An effective wavenumber  $1.1 \leq \nu_{\text{eff}} \leq 1.9$  for the five-parameter solution and  $1.24 \leq \text{pseudocolor} \leq 1.72$  for six-parameter solution.
- The spectral color  $0.3 < B_p - R_p < 1.65$  mag.

Only distant giant stars are selected for this study as shown in the first selection criterion. The systematic difference between  $M_{K_s}$  coming from Wang et al. (2022, accepted) and that estimated using the distance of Bailer-Jones et al. (2021) of our test sample are 0.015 mag and 0.0049 mag for dwarf and giant stars as shown in Fig.1, respectively (Wang et al. 2022, accepted). Because the typical parallaxes of the dwarf and giant stars in our sample are 1.5 and 0.45 mas, respectively, these systematic differences in  $M_{K_s}$  will typically produce a systematic parallax difference of about  $\sim 10.3 \mu\text{as}$  for the dwarf stars, and  $\sim 1.0 \mu\text{as}$  for the giants. Furthermore, the effect of binary stars on the estimated absolute magnitudes of dwarf stars is larger than that of giant stars. Thus, we only select distant giant stars as tracers to check the zero-point offset of Gaia EDR3 parallax in the current work. The RUWE is a quality indicator of Gaia EDR3 data, given by the renormalized square root of the reduced chisquare of the Gaia astrometric solution. Larger values indicate that the astrometric solution does not completely describe the source motion (Lindegren et al. 2021a; Fabricius et al. 2021). The stars with large value of RUWE are also removed. The effective wavenumber and pseudocolor represent the color information of the observed targets. Besides, the stars with  $B_p - R_p \leq 0.3$  mag or  $B_p - R_p \geq 1.65$  mag are also removed in order to make sure that our training sample could cover all kinds of stars in our giant sample (one can see Section 2.2 for more details). After the above cuts, we select about 268,003 and 5,070 LAMOST giant stars with five-parameter and six-parameter solutions in Gaia EDR3, respectively.

### 2.2. The parallax quality of our giant sample

As shown in Wang et al. (2022, accepted), the photometric distance are estimated with the distance modulus method using the 2MASS  $K_s$  band apparent magnitudes, interstellar extinctions and  $M_{K_s}$  derived directly from the LAMOST spectra. Amongst of them, the  $M_{K_s}$  are derived using neural network models, which are built up using the LGMWAS (LAMOST-Gaia EDR3-2MASS-WISE-APASS-SDSS) common stars as training set. In the LGMWAS training sample, the absolute magnitudes are estimated using the geometrical Gaia EDR3 distance (Bailer-Jones et al.

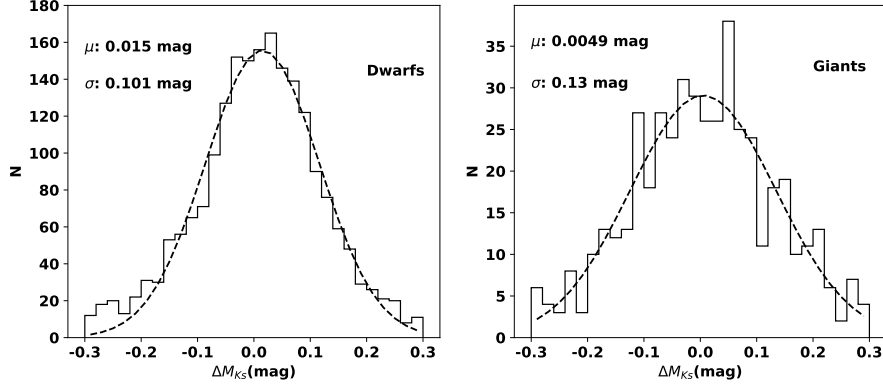


**Figure 1.** The distributions of  $M_{K_s}$  difference between  $M_{K_s}$  coming from Wang et al. (2022, accepted) ( $M_{K_s}^W$ ) and that estimated using the distance of Bailer-Jones et al. (2021) ( $M_{K_s}^{Gaia}$ ) of the test sample in Wang et al. (2022, accepted). The left and right panels are the results of dwarfs and giants, respectively. The black dashed line represent Gaussian fits for the difference distributions. The mean values and standard deviations of the two distributions are labeled in the top left corner of each panel. The  $\Delta M_{K_s}$  is the  $M_{K_s}^{Gaia} - M_{K_s}^W$ .

2021), based on the Gaia EDR3 parallaxes corrected according to Lindegren et al. (2021b). We can nevertheless use the distances in Wang et al. (2022, accepted) to test the parallax bias in Gaia EDR3 because the mean parallax of the LGMWAS training set ( $\sim 2$  mas) is much larger than the mean parallax in our giant sample ( $\sim 0.45$  mas). Our sample is therefore 4–5 times more sensitive to a parallax bias than the training set, which breaks the degeneracy, considering also that the two samples cover the same ranges of absolute magnitude and spectral color as shown in Fig. 2.

In Wang et al. (2022, accepted), we only select stars with small extinctions ( $E(B - V) < 0.02$  mag) as training stars. Almost all of our giant stars have larger extinction (with a median value of  $E(B - V) \sim 0.09$  mag, estimated using “star-pair” method of Yuan et al. (2013)) and extinction errors (with a typical value of 0.02 mag) than that of training stars, which will produce larger errors of the estimated photometric distance. The uncertainties of 0.006 mag for the 2MASS  $K_s$  band apparent magnitude and  $1.2 \mu\text{as}$  for the the estimated parallax will be caused by the typical extinction error. This parallax error is very small even if it is a systematic error. Thus, the variations of estimated parallax zero-point offset with spectral color, apparent magnitude and spatial positions will be less affected considering also the huge number of stars in our giant sample. In conclusion, although the estimates of parallax in our giant sample are based on the geometrical Gaia EDR3 distance of Bailer-Jones et al. (2021), we could use the sample to test the parallax bias of Gaia EDR3 and its dependence on the spectral color, apparent magnitude and spatial positions.

PRC stars are standard candles, their absolute magnitudes and distances could be accurately estimated (Cannon 1970; Paczyński & Stanek 1998; Bovy et al. 2014; Huang et al. 2015; Wan et al. 2015; Chen et al. 2017; Huang et al. 2020). Huang et al. (2020) have selected  $\sim 140,000$  PRCs from LAMOST, the distances of which could be accurate to 5% for stars with spectral SNRs larger than 50. We cross-match our giant sample and PRC sample of Huang et al. (2020), and select 49,459 common stars. Fig. 3 shows the comparison of our parallax ( $\omega_G$ ) and PRC parallax ( $\omega_{RC}$ ) and the parallax difference variations with the PRC parallax. The global systematic difference of the two kinds of parallax is  $3.6 \mu\text{as}$ , which is slightly larger than the claimed typical parallax systematic difference ( $\sim 1.0 \mu\text{as}$ ) between our parallax and official zero-point offset corrected Gaia EDR3 parallax as discussed in the Section 2.1. It is reasonable considering the systematic difference between the corrected Gaia EDR3 parallax and the parallax of PRC sample. The standard deviation of the parallax difference is  $\sim 41 \mu\text{as}$ , which is also good enough. From Fig. 3, we can find a trend of parallax difference with the parallax. The parallax difference are  $-1\%$ ,  $1\%$  and  $3\%$  at  $\omega_{RC} \sim 200 \mu\text{as}$  (corresponding parallax error is  $\sim -2 \mu\text{as}$ ),  $\omega_{RC} \sim 450 \mu\text{as}$  (corresponding parallax error is  $\sim +4.5 \mu\text{as}$ ) and  $\omega_{RC} \geq 1000 \mu\text{as}$  (corresponding parallax error is  $\geq +30 \mu\text{as}$ ), respectively. Considering the typical parallax of our giant stars is  $\sim 450 \mu\text{as}$ , the several  $\mu\text{as}$  systematic error of our giant sample and its variations with parallax will produce small systematic error of our final estimated parallax zero-point offset, which are supported by the similar global parallax zero-point offsets of us and other previous works discussed in Section 3. Besides, the stars with different parallax have similar spatial distributions, which suggest that the relative spatial variations of the estimated parallax zero-point offset will not be affected by the

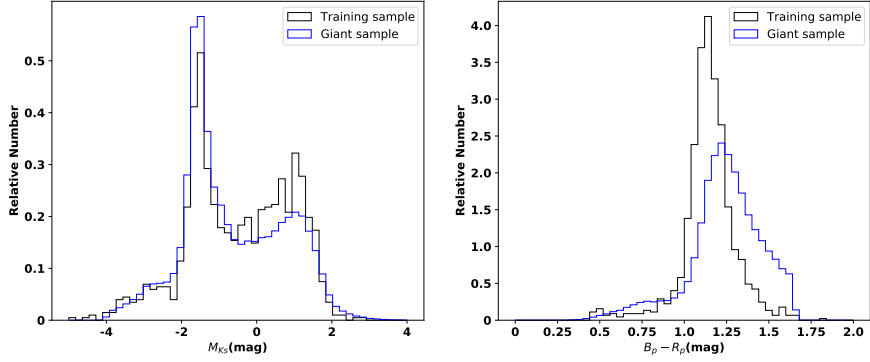


**Figure 2.** The absolute magnitude (left panel) and spectral color (right panel) distributions of the LGMWAS training sample (black lines) and our final giant sample (blue lines).

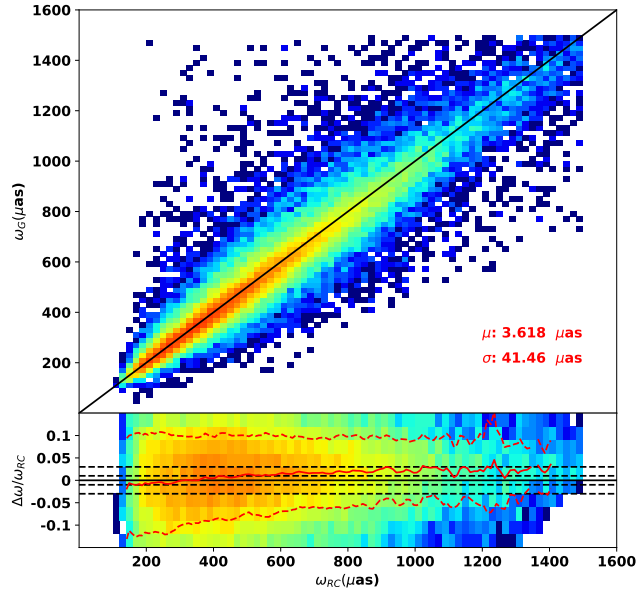


**Figure 3.** Top panel: the comparison between our parallax and PRC parallax. Bottom panel: the variations of relative parallax difference between our parallax and PRC parallax with the PRC parallax. The black dashed lines in the bottom panel are zero minus/plus 1% or 3%.

trend. In conclusion, our giant sample is a good sample to test the Gaia EDR3 parallax zero-point offset, especially its variations with apparent magnitude, spectral color and spatial positions.

In the current paper,  $\omega_{\text{EDR3}}$ ,  $\omega_{\text{EDR3}}^{\text{corr}}$  and  $\omega_{\text{G}}$  (here 'G' mean giant stellar sample) are the Gaia EDR3 parallax, Gaia EDR3 parallax with zero-point correction using the model of [Lindegren et al. \(2021b\)](#) and the parallax given by photometric distance of our LAMOST giant stars, respectively.

### 3. RESULTS AND DISCUSSIONS

Using the selected giant stars, we compare the parallaxes derived from our photometric distances ( $\omega_{\text{G}}$ ) with those from Gaia EDR3 ( $\omega_{\text{EDR3}}$ ) for the five- and six-parameter solutions. As shown in Fig. 4, the median offsets of Gaia EDR3 parallaxes are respectively  $-27.9 \mu\text{as}$  and  $-26.5 \mu\text{as}$  for the five- and six-parameter solutions, which are slightly larger than the value of  $-17 \mu\text{as}$  derived from distant quasars ([Lindegren et al. 2021b](#)). Our estimated median offsets are consistent with that of [Huang et al. \(2021\)](#),  $\sim -26 \mu\text{as}$  for both five- and six-parameter solutions) and [Ren et al.](#)

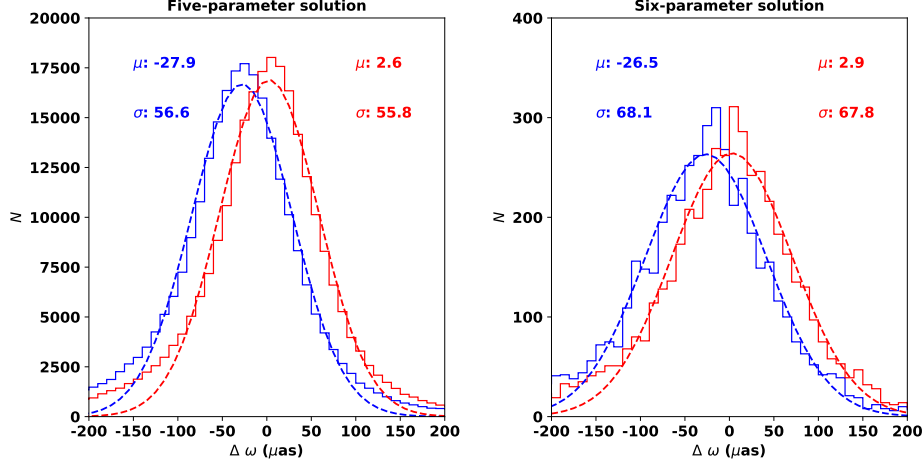


**Figure 4.** Differences distributions of parallaxes between the LAMOST giant stellar sample and Gaia EDR3 five-parameter solution (left panel) or six-parameter solution (right panel). The blue and red histograms represent the  $\omega_{\text{EDR3}} - \omega_{\text{G}}$  and  $\omega_{\text{EDR3}}^{\text{corr}} - \omega_{\text{G}}$  distributions, respectively. The blue and red dashed lines represent Gaussian fits for the two parallax difference distributions, respectively. The mean values and standard deviations of the two distributions are labeled in the top corner using their corresponding colors.

(2021,  $\sim -28$  and  $-25 \mu\text{as}$  for respectively five- and six-parameter solutions). The median values of the parallax difference between  $\omega_{\text{EDR3}}^{\text{corr}}$  and  $\omega_{\text{G}}$  are only  $+2.6$  and  $+2.9 \mu\text{as}$  for the five- and six-parameter solutions, respectively. The negligible positive values of median offsets suggest that the official parallax zero-point correction model (Lindgren et al. 2021b) significantly reduces the global bias of Gaia EDR3 parallaxes.

As discussed in Lindgren et al. (2021b), Huang et al. (2021) and Ren et al. (2021), the bias of Gaia EDR3 parallaxes is dependent on apparent magnitude ( $G$  band), effective wavenumber  $\nu_{\text{eff}}$ /pseudocolor and ecliptic latitude ( $\sin\beta$ ). With the advantage of large number of stars, large and continue coverage in the Galactic plane and wide range of colors and magnitudes of our giant sample, we test the main dependencies of the Gaia EDR3 parallaxes bias. Fig. 5 shows the parallax bias of  $\omega_{\text{EDR3}} - \omega_{\text{G}}$  and  $\omega_{\text{EDR3}}^{\text{corr}} - \omega_{\text{G}}$ , as a function of  $G$  magnitude, effective wavenumber  $\nu_{\text{eff}}$ /pseudocolor, ecliptic latitude  $\sin\beta$  for the five- and six-parameter solutions. From Fig. 5, we find that the  $\omega_{\text{EDR3}} - \omega_{\text{G}}$  are almost  $-30 \mu\text{as}$ , the  $\omega_{\text{EDR3}}^{\text{corr}} - \omega_{\text{G}}$  are almost  $0 \mu\text{as}$ , which is similar with the result shown in Fig. 4.

From Fig. 5, we can find significant patterns of  $\omega_{\text{EDR3}} - \omega_{\text{G}}$  as a function of  $G$  magnitude for both five- and six-parameter solutions. The “hump-like” feature in  $10 < G < 11$  and  $12 < G < 13$  are found for both five- and six-parameter solutions, which is similar with the results of Lindgren et al. (2021b) and Huang et al. (2021). The  $\omega_{\text{EDR3}}^{\text{corr}} - \omega_{\text{G}}$  are almost equal to zero and show smaller variations with  $G$  magnitude. The results suggest that the official parallax zero-point correction could reduce parallax bias patterns with  $G$  magnitudes. The  $\omega_{\text{EDR3}} - \omega_{\text{G}}$  and  $\omega_{\text{EDR3}}^{\text{corr}} - \omega_{\text{G}}$  as a function of  $\nu_{\text{eff}}$ / pseudocolour show several patterns for five- or six-parameter solutions, respectively. The results suggest that the official parallax zero-point correction could not reduce parallax bias patterns with spectral colors. For the  $\omega_{\text{EDR3}} - \omega_{\text{G}}$  and  $\omega_{\text{EDR3}}^{\text{corr}} - \omega_{\text{G}}$  variations with  $\sin\beta$ , we do not find significant trend for both five- and six-parameter solutions.

The bias of Gaia EDR3 parallax is positional dependent (Lindgren et al. 2021b; Huang et al. 2021; Ren et al. 2021). Our LAMOST giant sample covers a large and continue volume of the Galaxy and has huge number of stars, thus it is a better sample to investigate the distribution of the parallax biases as a function of spatial positions. Fig. 6 shows the maps of the mean parallax differences for the five-parameter solutions of  $\omega_{\text{EDR3}} - \omega_{\text{G}}$  and  $\omega_{\text{EDR3}}^{\text{corr}} - \omega_{\text{G}}$  in equatorial coordinates and Galactic coordinates. The  $\omega_{\text{EDR3}} - \omega_{\text{G}}$  are smaller than 0 at almost all position bins, with a median value of  $\sim -30 \mu\text{as}$ . The  $\omega_{\text{EDR3}}^{\text{corr}} - \omega_{\text{G}}$  are smaller than  $+30 \mu\text{as}$  and larger than  $-30 \mu\text{as}$  at almost all position bins, with a median value of  $\sim 0 \mu\text{as}$ . The results suggest that the official corrections for Gaia EDR3 parallaxes are effective in reducing global offset in the Gaia parallaxes. From this plot, we find that the Gaia EDR3 parallax bias exhibit significant and clear trend with the positions. The parallax biases in the Galactic plane ( $b \sim 0^\circ$ ) are largest, which is similar with the result of Lindgren et al. (2021b) and Ren et al. (2021). Fig. 6 suggests that the parallax biases

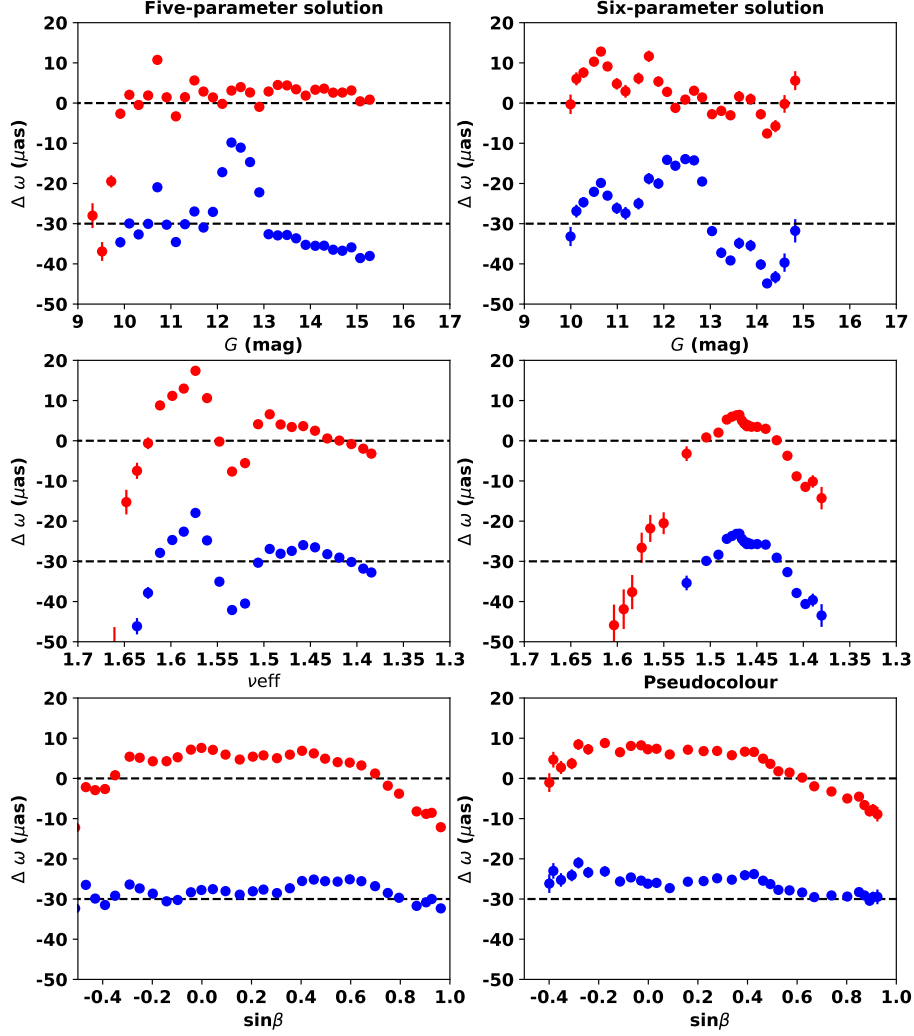


**Figure 5.** Parallax differences between our LAMOST giant sample and Gaia EDR3 five-parameter solution (left panel) or Gaia EDR3 six-parameter solution (right panel), as a function of  $G$  band magnitudes (top panels), color information (middle panels:  $\nu_{\text{eff}}$  for five-parameter solution, pseudocolour for six-parameter solution) and ecliptic latitude  $\sin\beta$  (bottom panels). The blue and red points represent the  $(\omega_{\text{EDR3}} - \omega_{\text{G}})$  and  $(\omega_{\text{EDR3}}^{\text{corr}} - \omega_{\text{G}})$ , respectively. In each bin, the number of stars is no less than 100. The black dashed lines in each panel mark the differences of  $-30 \mu\text{as}$  and  $0 \mu\text{as}$ .

before and after correction show similar trends with the positions, which suggest that official correction for Gaia EDR3 parallaxes could not reduce the parallax bias variations with positions. A spatially dependent Gaia EDR3 parallax zero-point correction model is needed.

We will provide a dataset, which contains the position-dependent Gaia EDR3 parallax zero-point corrections for five-parameter solution within the LAMOST footprint in the Galactic coordinate and equatorial coordinate. The resolution of each pixel is about  $3.36 \text{ deg}^2$  in HEALPix (Hierarchical Equal Area isoLatitude Pixelisation; Górski et al. 2005) grid after dividing the whole sky into 12288 equal area pixels, which is same with that in Fig.6. For the stars located in a pixel we obtain the mean ( $\mu$ ) and standard deviation ( $\sigma$ ) of  $\omega_{\text{EDR3}} - \omega_{\text{G}}$  and  $\omega_{\text{EDR3}}^{\text{corr}} - \omega_{\text{G}}$  by



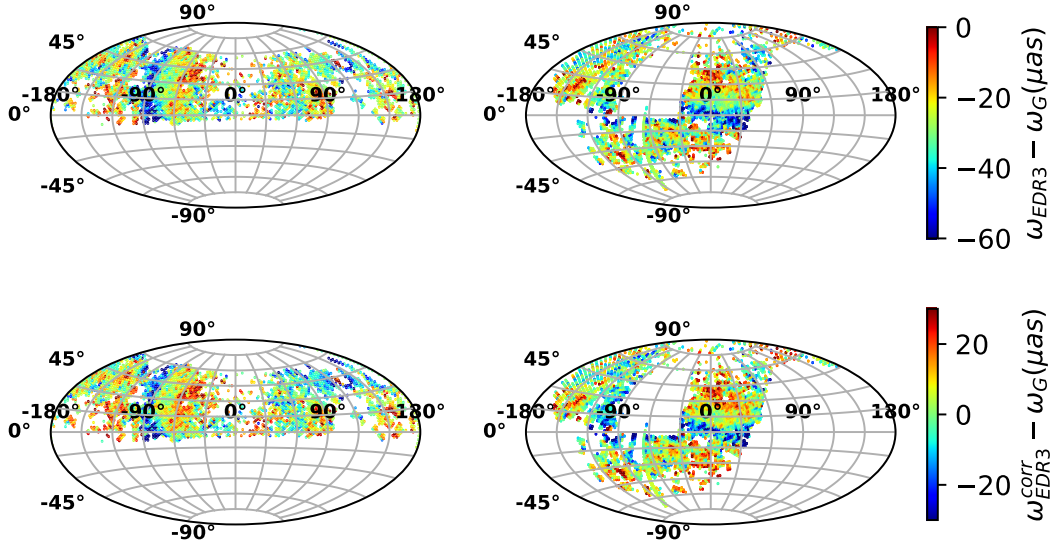


**Figure 6.** Maps of  $\omega_{\text{EDR3}} - \omega_{\text{G}}$  (top panels) and  $\omega_{\text{EDR3}}^{\text{corr}} - \omega_{\text{G}}$  (bottom panels) in equatorial coordinate (left panels) and Galactic coordinate (right panels) for the five-parameter solutions. Each pixel covers equal sky area of about 3.36 square degrees. Number of stars in each pixel is larger than 50.

**Table 1.** Descriptions for the dataset to correct spatially dependent Gaia EDR3 parallax zero-point offset for five-parameter solutions.

Field	Description	Unit
hindex	the HEALPix index number (level 5)	-
ra	Right ascension at the center of each pixel	degree
dec	Declination at the center of each pixel	degree
gl	Galactic longitude at the center of each pixel	degree
gb	Galactic latitude at the center of each pixel	degree
$\Delta\omega^{\text{corr}}$	$\omega_{\text{EDR3}}^{\text{corr}} - \omega_{\text{G}}$ values in each pixel	$\mu\text{as}$
$E.\Delta\omega^{\text{corr}}$	the error of estimated $\Delta\omega^{\text{corr}}$ in each pixel	$\mu\text{as}$
$\Delta\omega^{\text{noncorr}}$	$\omega_{\text{EDR3}} - \omega_{\text{G}}$ values in each pixel	$\mu\text{as}$
$E.\Delta\omega^{\text{noncorr}}$	the error of estimated $\Delta\omega^{\text{noncorr}}$ in each pixel	$\mu\text{as}$
$N$	Number of stars in each pixel	-

fitting a gaussian function. The dataset gives for each pixel  $\mu$  as the Gaia EDR3 parallax zero-point correction in the pixel,  $\frac{\sigma}{\sqrt{N}}$  as the corresponding error, and  $N$  as the number of stars in the pixel. One can use this dataset to correct the spatially dependent Gaia EDR3 parallax zero-point offset. The dataset will be released in the website of <http://www.lamost.org/dr8/v1.0/doc/vac>. Table. 1 shows the detailed description of the dataset. It is noted that we give both the position-dependent Gaia EDR3 parallax zero-point corrections in the Galactic and equatorial coordinates, one can choose one of them according to their coordinates.

#### 4. SUMMARY

In the current paper, we use  $\sim 0.3$  million giant stars selected from the LAMOST to investigate the zero-point offset of the Gaia EDR3 parallax  $\omega_{\text{EDR3}}$  and the Gaia EDR3 parallax after correction  $\omega_{\text{EDR3}}^{\text{corr}}$  using the model of Lindegren et al. (2021b). The distance accuracy of these giant stars are about 8.5%. The global median zero-point offset of  $\omega_{\text{EDR3}}$  are  $-27.9 \mu\text{as}$  and  $-26.5 \mu\text{as}$  for five-parameter solution and six-parameter solution, respectively. The bias of  $\omega_{\text{EDR3}}^{\text{corr}}$  are  $+2.6 \mu\text{as}$  and  $+2.9 \mu\text{as}$  for five-parameter solution and six-parameter solution, respectively.

We also studied the main dependences of the Gaia EDR3 parallax bias before and after correction. We find that the parallax bias show significant systematic trends with  $G$  magnitude, spectral colors. The official parallax zero-point correction could reduce the global offset in the Gaia EDR3 parallaxes and the significant systematic trends with  $G$  magnitude. While the official parallax zero-point correction could not reduce the parallax bias variations with spectral colors. With the advantage of the huge number of stars in our giant stellar sample, we also investigate the parallax bias variations with positions. Both the parallax bias before and after correction exhibit significant and clear trend with the positions, which suggest that the official parallax zero-point correction could not reduce the parallax bias variations with positions. In the current paper, a spatially dependent Gaia EDR3 parallax zero-point correction model for five-parameter solutions in the LAMOST footprint is firstly provided.

This work was funded by the National Key R&D Program of China (No. 2019YFA0405500) and the National Natural Science Foundation of China (NSFC Grant No.11833006, U1531244 and 11973001, 12173007). We used data from the European Space Agency mission Gaia (<http://www.cosmos.esa.int/gaia>), processed by the Gaia Data Processing and Analysis Consortium (DPAC; see <http://www.cosmos.esa.int/web/gaia/dpac/consortium>). Guoshoujing Telescope (the Large Sky Area Multi-Object Fiber Spectroscopic Telescope LAMOST) is a National Major Scientific Project built by the Chinese Academy of Sciences. Funding for the project has been provided by the National Development and Reform Commission. LAMOST is operated and managed by the National Astronomical Observatories, Chinese Academy of Sciences.

## REFERENCES

- Bailer-Jones, C. A. L., Rybizki, J., Fouesneau, M., Demleitner, M., & Andrae, R. 2021, *VizieR Online Data Catalog*, I/352
- Bhardwaj, A., Rejkuba, M., de Grijs, R., et al. 2021, *ApJ*, 909, 200, doi: [10.3847/1538-4357/abdf48](https://doi.org/10.3847/1538-4357/abdf48)
- Bovy, J., Nidever, D. L., Rix, H.-W., et al. 2014, *ApJ*, 790, 127, doi: [10.1088/0004-637X/790/2/127](https://doi.org/10.1088/0004-637X/790/2/127)
- Cannon, R. D. 1970, *MNRAS*, 150, 111, doi: [10.1093/mnras/150.1.111](https://doi.org/10.1093/mnras/150.1.111)
- Chen, Y. Q., Casagrande, L., Zhao, G., et al. 2017, *ApJ*, 840, 77, doi: [10.3847/1538-4357/aa6d0f](https://doi.org/10.3847/1538-4357/aa6d0f)
- Deng, L.-C., Newberg, H. J., Liu, C., et al. 2012, *Research in Astronomy and Astrophysics*, 12, 735, doi: [10.1088/1674-4527/12/7/003](https://doi.org/10.1088/1674-4527/12/7/003)
- El-Badry, K., Rix, H.-W., & Heintz, T. M. 2021, *MNRAS*, 506, 2269, doi: [10.1093/mnras/stab323](https://doi.org/10.1093/mnras/stab323)
- Fabricius, C., Luri, X., Arenou, F., et al. 2021, *A&A*, 649, A5, doi: [10.1051/0004-6361/202039834](https://doi.org/10.1051/0004-6361/202039834)
- Gaia Collaboration, Prusti, T., de Bruijne, J. H. J., et al. 2016, *A&A*, 595, A1, doi: [10.1051/0004-6361/201629272](https://doi.org/10.1051/0004-6361/201629272)
- Gaia Collaboration, Brown, A. G. A., Vallenari, A., et al. 2021, *A&A*, 649, A1, doi: [10.1051/0004-6361/202039657](https://doi.org/10.1051/0004-6361/202039657)
- Górski, K. M., Hivon, E., Banday, A. J., et al. 2005, *ApJ*, 622, 759, doi: [10.1086/427976](https://doi.org/10.1086/427976)
- Groenewegen, M. 2021, arXiv e-prints, arXiv:2106.08128. <https://arxiv.org/abs/2106.08128>
- Huang, Y., Yuan, H., Beers, T. C., & Zhang, H. 2021, *ApJL*, 910, L5, doi: [10.3847/2041-8213/abe69a](https://doi.org/10.3847/2041-8213/abe69a)
- Huang, Y., Liu, X.-W., Zhang, H.-W., et al. 2015, *Research in Astronomy and Astrophysics*, 15, 1240, doi: [10.1088/1674-4527/15/8/010](https://doi.org/10.1088/1674-4527/15/8/010)
- Huang, Y., Schönrich, R., Zhang, H., et al. 2020, *ApJS*, 249, 29, doi: [10.3847/1538-4365/ab994f](https://doi.org/10.3847/1538-4365/ab994f)
- Liao, S., Wu, Q., Qi, Z., et al. 2021, *PASP*, 133, 094501, doi: [10.1088/1538-3873/ac1eeb](https://doi.org/10.1088/1538-3873/ac1eeb)
- Lindegren, L., Klioner, S. A., Hernández, J., et al. 2021a, *A&A*, 649, A2, doi: [10.1051/0004-6361/202039709](https://doi.org/10.1051/0004-6361/202039709)
- Lindegren, L., Bastian, U., Biermann, M., et al. 2021b, *A&A*, 649, A4, doi: [10.1051/0004-6361/202039653](https://doi.org/10.1051/0004-6361/202039653)
- Liu, X.-W., Yuan, H.-B., Huo, Z.-Y., et al. 2014, in *IAU Symposium*, Vol. 298, *IAU Symposium*, ed. S. Feltzing, G. Zhao, N. A. Walton, & P. Whitelock, 310–321, doi: [10.1017/S1743921313006510](https://doi.org/10.1017/S1743921313006510)
- Paczyński, B., & Stanek, K. Z. 1998, *ApJL*, 494, L219, doi: [10.1086/311181](https://doi.org/10.1086/311181)
- Ren, F., Chen, X., Zhang, H., et al. 2021, *ApJL*, 911, L20, doi: [10.3847/2041-8213/abf359](https://doi.org/10.3847/2041-8213/abf359)



- Skrutskie, M. F., Cutri, R. M., Stiening, R., et al. 2006, *AJ*, 131, 1163, doi: [10.1086/498708](https://doi.org/10.1086/498708)
- Stassun, K. G., & Torres, G. 2021, *ApJL*, 907, L33, doi: [10.3847/2041-8213/abdaad](https://doi.org/10.3847/2041-8213/abdaad)
- Wan, J.-C., Liu, C., Deng, L.-C., et al. 2015, *Research in Astronomy and Astrophysics*, 15, 1166, doi: [10.1088/1674-4527/15/8/006](https://doi.org/10.1088/1674-4527/15/8/006)
- Yuan, H. B., Liu, X. W., & Xiang, M. S. 2013, *MNRAS*, 430, 2188, doi: [10.1093/mnras/stt039](https://doi.org/10.1093/mnras/stt039)
- Zhao, G., Zhao, Y.-H., Chu, Y.-Q., Jing, Y.-P., & Deng, L.-C. 2012, *Research in Astronomy and Astrophysics*, 12, 723, doi: [10.1088/1674-4527/12/7/002](https://doi.org/10.1088/1674-4527/12/7/002)
- Zinn, J. C. 2021, *AJ*, 161, 214, doi: [10.3847/1538-3881/abe936](https://doi.org/10.3847/1538-3881/abe936)